



## Promising Potential of Electro-Coagulation Process for Effective Treatment of Biotreated Palm Oil Mill Effluents

Amina Tahreen<sup>1</sup>, Mohammed Saedi Jami<sup>1\*</sup>, Fathilah Ali<sup>1</sup>, Nik Mohd Farid Mat Yasin<sup>2</sup> and Mohammed Ngabura<sup>3</sup>

1. Department of Biotechnology Engineering, Faculty of Engineering, International Islamic University Malaysia, P.O Box 10, 50728 Kuala Lumpur, Malaysia

2. Processing & Engineering, Sime Darby Plantation Research Sdn Bhd, 42960 Selangor, Malaysia

3. Department of Chemical and Environmental Engineering, Faculty of Engineering, University Putra Malaysia, 43400 Serdang, Selangor, Malaysia

Received: 14 February 2021, Revised: 28 April 2021, Accepted: 01 July 2021

© University of Tehran

### ABSTRACT

The critical parameters namely initial pH, time and current density largely impact the process efficiency of electrocoagulation (EC). Few works have been done on observing the interaction of these critical parameters and the possible combined effect on the overall pollutant removal efficiency. Therefore, the knowledge of the combined effect of critical parameter interaction would enhance the optimization of EC parameters to attain maximum efficiency with limited resources. Using aluminium electrodes with interelectrode distance of 10 mm on synthetic wastewater, representing biotreated palm oil mill effluent (BPOME), with a set range of initial pH, current density, and time of 3-8, 40-160 mA/cm<sup>2</sup> and 15 to 60 minutes, respectively, the effect of the three critical variables was investigated. The optimum Chemical Oxygen Demand (COD) removal of 71.5% was determined at pH 6, current density of 160 mA/cm<sup>2</sup> (with current 1.75 A) at EC time of 15 minutes. The experiment was validated with real BPOME, resulting in the removal efficiency of 60.7 % COD, 99.91 % turbidity, 100 % total suspended solids (TSS) and 95.7 % colour. Removal of a large quantity of pollutants in a time span of 15 minutes with optimized parameters in EC is notable for a wastewater treatment alternative that requires no extensive use of chemicals. The interaction of parameters observed in this study indicated a synergistic contribution of initial pH and current density in removing maximum wastewater COD in 15 minutes of EC.

**KEYWORDS:** Wastewater treatment, Industrial effluent, Optimization, Parameter interaction

### INTRODUCTION

With leaps in global advancements in industrial development, fresh water crisis is a rapid rising concern. The magnified concerns had been highlighted by World Economic Forum (WEF), with a prediction of economic deterioration due to fresh water decline (WEF, 2020). Moreover, the United Nations (UN) has placed Sustainable Development Goal (SDG) 6, to accomplish increase in reduction in wastewater emissions, and reclamation for safe industrial

\* Corresponding Author, Email: saedi@iium.edu.my

reuse (UN, 2018). Therefore, there is a need for an effective water treatment system that can sustainably treat and reclaim reusable water from industrial effluents.

A frequently used wastewater treatment is chemical coagulation-flocculation (Jawad et al., 2016), with underlying drawbacks of continuous chemical intensive process, production of increased sludge quantity and acidified final treated water (Bannari et al., 2019). Besides, adsorption (Jayakaran et al., 2019), advanced oxidation process (AOP) (Bahadur & Bhargava, 2019; Boczkaj & Fernandes, 2017) and membrane technology (Amosa et al., 2016; Ilyas et al., 2020) displayed effective treatment performance but most of these processes incur a high cost. Electrocoagulation (EC) stands out to be an effective alternative to these processes. EC is an electrochemical treatment that is inexpensive, easy to maintain, has no moving parts, does not require harsh chemicals, and therefore, is environmentally friendly (Moussa et al., 2017; Tahreen et al., 2020). The resulting sludge produced in EC process is less in quantity compared to that of other wastewater treatment plants. Moreover, the EC sludge generated over time can be utilized to convert into clay bricks (Thakur et al., 2019) or utilized for renewable biomaterial production (Aslan et al., 2016), thus, paving way towards a zero-waste water reclamation system.

EC involves continuous generation of metal ions in situ by applying a constant current that forms coagulants that destabilizes the pollutants and cause them to form flocs that are separated by flotation and decantation (Bannari et al., 2019). It has been increasingly studied as a pre-treatment process for membrane technologies for wastewater treatment and reclamation (Tahreen & Jami, 2021). It is a versatile process and is studied on many types of wastewater involving various types of pollutants, such as tannery wastewater (Deveci et al., 2019), leachate wastewater (Sediqi et al., 2021), arsenic and fluoride based wastewater (Sandoval et al., 2021), pharmaceutical wastewater (Zaied et al., 2020), dairy processing and slaughterhouse wastewater (Reilly et al., 2019), bilge water (Akarsu et al., 2016), laundry wastewater (Dimoglo et al., 2019) and biodiesel wastewater (Chavalparit & Ongwande, 2009). Aluminium and iron are widely used as electrodes for EC, due to their ease of availability, low cost and ability to generate multivalent metal ions on current application. Many researchers preferred aluminium over iron as EC electrodes due to reduced complexities from dual oxidation states of iron (Tahreen et al., 2020). Therefore, aluminium was employed in this study, and the redox reactions involved in aluminium dissociation in EC are presented in the equations (5) and (6). The subsequent formation of aluminium hydroxides as coagulants begins the EC process by destabilizing the pollutant colloids, followed by flocculation.

There is a rising concern regarding the increased production of palm oil mill effluents (POME) from the oil palm industries. Current wastewater treatment processes such as biological treatments namely aerobic treatment, anaerobic and facultative pond effluent open decomposition tank and composting of organic fertilizer are the conventional treatments for palm oil mill effluents (POME) (Iskandar et al., 2018), requiring a large surface area and a very long retention time, producing a foul stench that becomes detrimental to the environmental well-being. The final discharged biotreated POME still contains a huge amount of organic matter, suspended solids and turbidity that hinders the marine life and the environment. Moreover, huge amount of water used in the palm oil production processes are lost as effluents.

Few studies reported an enhanced Chemical Oxygen Demand (COD) removal and shortened reaction time with EC on POME. Bashir et al. (2019) and Nasrullah et al. (2017) integrated EC process with additional oxidizing agent such as hydrogen peroxide ( $H_2O_2$ ). Nasrullah et al. (2017) introduced a coagulating aid namely polyaluminum chloride (PAC), in

addition to  $H_2O_2$ , to enhance the EC process to achieve better COD removal. Addition of strong oxidants stands as a drawback if an overall environment friendly process is aimed. It was observed that the COD removal % varied significantly with the additional coagulant in the EC process as compared to Bashir et al. (2019) but required longer residence time. By observing the effect of initial pH and optimization, the overall time required for the EC process can be minimized. For instance, Rusdianasari et al. (2017) monitored the effect of voltage and process time and achieved the optimum COD removal at 150 minutes. By considering the effect of initial pH and combined parametric effect on COD removal, the process time can be minimized, making the EC process more efficient.

Differences arise notably due to frequent changes in the POME effluent characteristics as the samples differ in characterization due to biodegradation and effluent quality fluctuation. Besides, the point of collection and biological post treatment of the POME samples employed in these studies were different. Therefore, to have a more solid understanding on the effectiveness of EC on removal of COD, a fully controlled synthetic wastewater was prepared in this research that closely represents biotreated POME. As a result, a more consistent and reliable outcome can be achieved, in terms of COD removal as a primary response. Hence, synthetic wastewater can be used to represent the actual biotreated POME to minimize the complications of the raw wastewater. Lack of microbial activity in the synthetic sample provides a nearly constant environment for the experiments, enabling the prolonged usability of the samples (Abdulazeez et al., 2018).

This study focuses on EC as an alternative post treatment process for biotreated POME and investigates its ability to sustainably reclaim process water for reuse in the industry. Biotreated POME, also known as BPOME, is the final discharge effluent of the palm oil industries, that holds the potential to be reused in the industry with a sustainable water reclamation system, mitigating fresh water scarcity and environmental pollution. Many researchers have studied the effect of operational parameters on EC efficiency. However, few studies are found that investigate the parameter interaction and the combined parametric effect on pollutant removal % with EC. Therefore, observing the effect of critical operating parameters namely current density, initial pH and time, and their combined effect on pollutant removal efficiency and EC optimization in this study, will propel the advancement of this sustainable technology in the palm oil industries. As another stepping stone for sustainably producing cleaner effluents for discharge and potential water reclamation, this study paves a way to the direction of accomplishing the SDG 6, aiming to reduce and reuse industrial effluents.

## MATERIALS AND METHODS

The synthetic wastewater having similar characteristics with BPOME, was prepared by adapting the artificial wastewater composition from (Nopens et al., 2001). It was characterized at room temperature ( $27^\circ C$ ) and the values are depicted in Table 1.

**Table 1.** Characterization of synthetic wastewater.

Parameters	Average values
COD (mg/L)	2449
Conductivity (mS/cm)	17.67
Salinity (ppt)	10.4
pH	5.65
TDS (g/L)	10
Turbidity (NTU)	328

Aluminium (Al) plates of dimensions 1.55 mm x 20 mm x 100 mm were rinsed with HCl and dried before the setup as electrodes. A 250 ml beaker was used as the EC cell connected to the DC supply (Twintex TP-2303K, Taiwan) via the electrodes. A schematic diagram for the experimental setup for the EC run is presented in Figure 1. The runs were varied in terms of initial pH (3-8), current density (40-160 mA/cm<sup>2</sup>) with current ranging from 0.44 A to 1.75 A, effective anode surface area of 10.93 cm<sup>2</sup>, and EC time (15-60 minutes) for optimization using design of experiment. The interelectrode distance was set constant to 10 mm (Aswathy et al., 2016; Hussin et al., 2017; Khosravi et al., 2017; McBeath et al., 2020). The challenge faced while running EC was the electrical conductivity of the synthetic wastewater. To enable the current flow based on the chosen current density range, the addition of NaCl as electrolyte was necessary, as the conductivity of the synthetic solution was not enough to apply the required current density. After a series of electrolyte additions and observation of current flow on synthetic wastewater, 10 g/L NaCl concentration was chosen and kept constant for all the batches of synthetic wastewater preparation so the maximum current density in this study's chosen range can be applied. The results obtained were optimized with Design Expert Software version 13.0, using Response Surface Methodology (RSM) technique. The considered factors were current density, pH and time denoted as *A*, *B* and *C*, respectively.

The experiments were carried out in room temperature (27 °C) and the synthetic wastewater was prepared, EC treated and tested for COD on the same day, to remove errors arising from possible COD degradation. Deionized water was used for all synthetic wastewater preparations. The Al electrodes were rinsed with 5% HCl solution before performing every run.

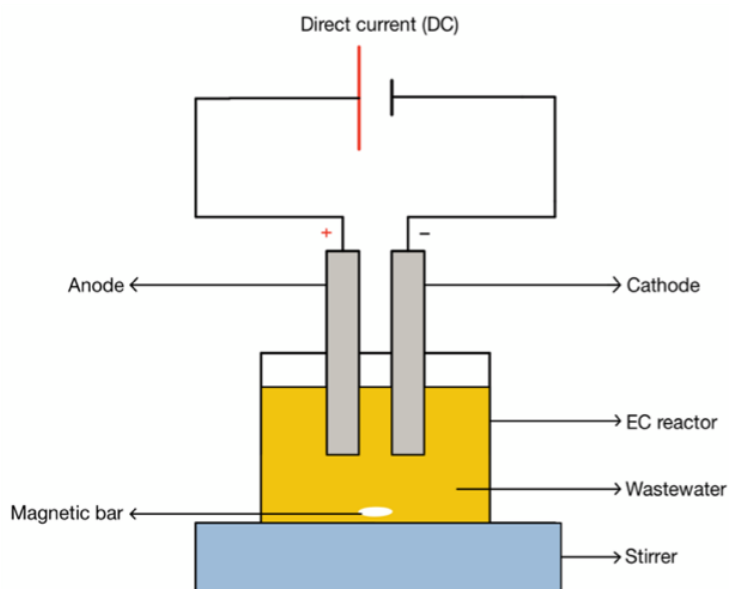


**Fig. 1.** Schematic diagram of simple EC setup

The wastewater samples were measured for COD, color and total suspended solids (TSS) before and after EC using spectrophotometer (HACH DR 5000, USA) according to American Public Health Association (APHA) standards (APHA, 2002). To control the initial pH of the samples, 5% HCl and 0.1M NaOH solutions and pH meter (Mettler Toledo, MP220 model, USA) were used. Multi-meter (HACH sensION5, USA) was used to measure the TDS, conductivity, and salinity of the wastewater samples. Turbidity of the samples were monitored with turbidimeter (HACH 2100P, USA). The aluminum anode was observed under scanning electron microscope (SEM) (JSM-IT100 version 1.060, Jeol, Japan).

## RESULT AND DISCUSSION

The resulting COD % removal values are stated in Table 2. COD % removal was calculated from equation (1):

$$\text{COD\% removal} = \frac{\text{COD (initial)} - \text{COD (final)}}{\text{COD (initial)}} \times 100\% \quad (1)$$

**Table 2.** Completed DOE table with COD removal % as response.

Run	Factor A Current density, mA/cm <sup>2</sup>	Factor B Initial pH	Factor C Time, min	Response COD removal, %
1	100	8	60	58.8
2	160	8	37.5	60
3	160	5.5	15	76.09
4	100	5.5	37.5	65
5	100	3	60	48.35
6	160	5.5	60	64.13
7	100	8	15	45.05
8	40	8	37.5	52.75
9	40	3	37.5	37.36
10	100	3	15	35.16
11	40	5.5	60	67.39
12	40	5.5	15	55
13	100	5.5	37.5	71.5
14	160	3	37.5	41.76
15	100	5.5	37.5	60
16	100	5.5	37.5	70
17	160	8	60	72
18	100	5.5	37.5	69
19	160	3	15	54.2
20	40	3	60	54.25
21	40	8	15	45.83
22	160	3	15	54.17
23	100	5.5	37.5	50
24	160	8	15	46.38
25	100	5.5	37.5	55.3

The COD removal % as a response variable to variation in the parameters, namely current density, initial pH, and time in EC process was analysed with Design Expert Software using its powerful tool RSM. The Box-Behnken Design (BBD) suggested a total of 15 runs with 3 centre points. The resulting empirical model was augmented with 10 more additional points and backward reduction of highly insignificant factors for strengthening the significance and the predictability of the model. The response surface was a fit to second-order polynomial model represented by equation (2), where  $\beta_0$ ,  $\beta_i$ ,  $\beta_{ii}$  and  $\beta_{ij}$  represent the coefficients of regression for the intercept, linear, quadratic and the interaction terms respectively. The symbols  $X_i$  and  $X_j$  denote the coded values of the independent variables and  $k$  is the quantity of variables studied in the design. The symbol  $\varepsilon$  represents the error value.

$$Y = \beta_0 + \sum_{i=1}^k \beta_i X_i + \sum_{i=1}^k \beta_{ii} X_i^2 + \sum_{i=1}^{k-1} \sum_{j=i+1}^k \beta_{ij} X_i X_j + \varepsilon \quad (2)$$

The model  $F$  value was 17.13 implying the model was highly significant to a  $p$ -value less than 0.0001. The  $R^2$  and adjusted  $R^2$  of the significant model was 0.896 and 0.843 and the

predicted  $R^2$  was 0.687 which was reasonably in agreement with the adjusted  $R^2$  as the difference between the values was less than 0.2. The adequate precision of the model was 11.94 proving that the signal to noise ratio was high ( $> 4$ ). Therefore, it is in the acceptable range enabling the model suitable for navigation of the design space. Moreover, the model lack of fit  $F$ -value was 0.85, implying that it was not significant relative to the pure error and therefore, proved a very good fit of the model. The statistical analysis data have been summarized in Table 3.

**Table 3.** ANOVA and fit- statistics for the reduced quadratic model.

Source	Sum of Squares	df	Mean Square	F-Value	p-value	
Block	572.76	3	190.92			
<b>Model</b>	2168.62	7	309.8	17.13	< 0.0001	significant
A-Current density	180.6	1	180.6	9.99	0.007	
B-Initial pH	526.61	1	526.61	29.12	< 0.0001	
C-Time	180.94	1	180.94	10	0.0069	
AB	16.87	1	16.87	0.9329	0.3505	
AC	208.54	1	208.54	11.53	0.0043	
BC	17.46	1	17.46	0.9652	0.3426	
B <sup>2</sup>	1463.03	1	1463.03	80.89	< 0.0001	
<b>Residual</b>	253.2	14	18.09			
Lack of Fit	172.16	10	17.22	0.8497	0.6221	not significant
Pure Error	81.04	4	20.26			
<b>Cor Total</b>	2994.57	24				

R-squared=0.8955  
Adjusted R-squared=0.8432  
Predicted R-squared=0.6870  
Adeq precision=11.9420

The model can be represented empirically by equation (3) in terms of coded factors:

$$\text{COD removal \%} = 65.51 + 4.17A + 6.95B + 4.05C + 1.50 AB - 5.22 AC + 1.58 BC - 17.10B^2 \quad (3)$$

The coded factor-based equation can be employed to predict the response for given levels of each factor, where A, B and C represent the current density, initial pH, and time respectively. By default, the high and low factor levels are coded as +1 and -1 respectively. The coded equation helps to identify the relative influence of the factors by comparing the factor coefficients.

Figure 3, Figure 4 and Figure 5 depict the 3D surfaces and contour plots of the effect of parameter interaction with COD removal % as the response variable. As observed in the 3D graphs, the interaction between the parameters EC time and pH was significant compared to EC time - current density and pH - current density. The parabolic slopes of the graphs depict the peak performance of COD removal with respect to the pair of parameters in concern. All the three parameters current density, initial pH, and time are significant implying their strong impact on the response variable, proven by the statistical significance, with  $p$ -values less than 0.05 in Table 3. The quadratic model depicts the highest COD removal % that can be achieved while varying two parameters at once and leveraging their combined effect on COD removal, true for current density and time in this study.

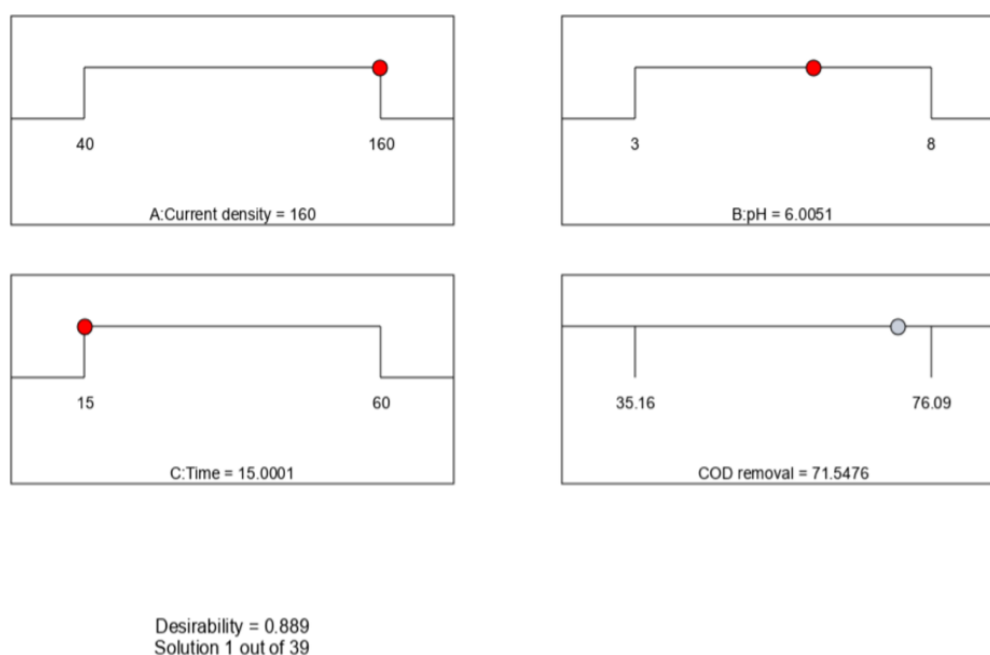


**Fig. 2.** Optimized variables depicted in ramps, generated using Design Expert 13.0.

With desirability value of 0.889, the optimized set of parameters was determined to be 160 mA/cm<sup>2</sup> (at 1.75 A), 6, and 15 minutes for current density, initial pH, and time respectively, for the optimum COD removal % of 71.5 as shown in Figure 2. These results correspond to the EC treatment on leachate by Sediqi et al. (2021), where the most cost consuming outcome (with minimum usage of electricity and materials) was achieved at pH 6, 3.4 A and 47 minutes. Under these conditions the highest COD removal observed was 51%. Therefore, relatively requiring a much lower current and time, a higher COD removal was observed in this work for the treatment of BPOME. The optimized numerical solution was validated with confirmation experiments in duplicates and the average COD removed was recorded to be 68.86% with a percentage error of 3.7 with the suggested COD % removal from the optimization solution.

The final EC treated effluent was characterized to observe the removal efficiencies of COD, TSS, turbidity, and colour, and the details are summarized in Table 4.

**Table 4.** Characterization of synthetic wastewater.

Parameters	Value	Average removal efficiency
COD (mg/L)	952.5	68.86%
TSS (mg/L)	0.5	99.68%
Color (PtCo)	15	97.95%
Turbidity (NTU)	2	99.39%

The combined effect of both current density and time in COD removal is visualised in the 3D and contour plots in Figure 3, Figure 4 and Figure 5. The interaction between current density and time is statistically significant in the response, with a p-value less than 0.05 compared to the combined effect of other parameters on COD removal % as shown in Table 3.

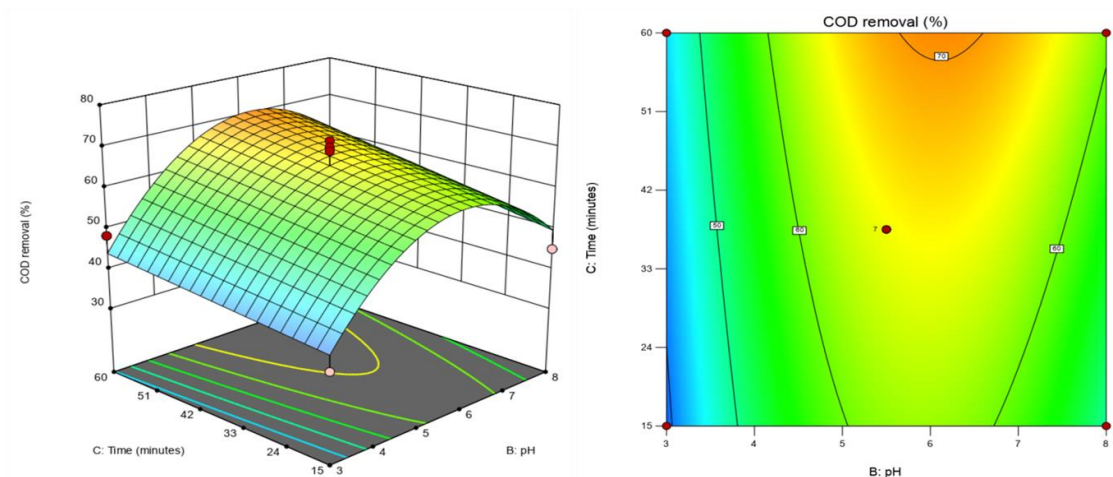


**Fig. 3.** 3D surface and contour plots showing the combined effect of time and initial pH on COD removal

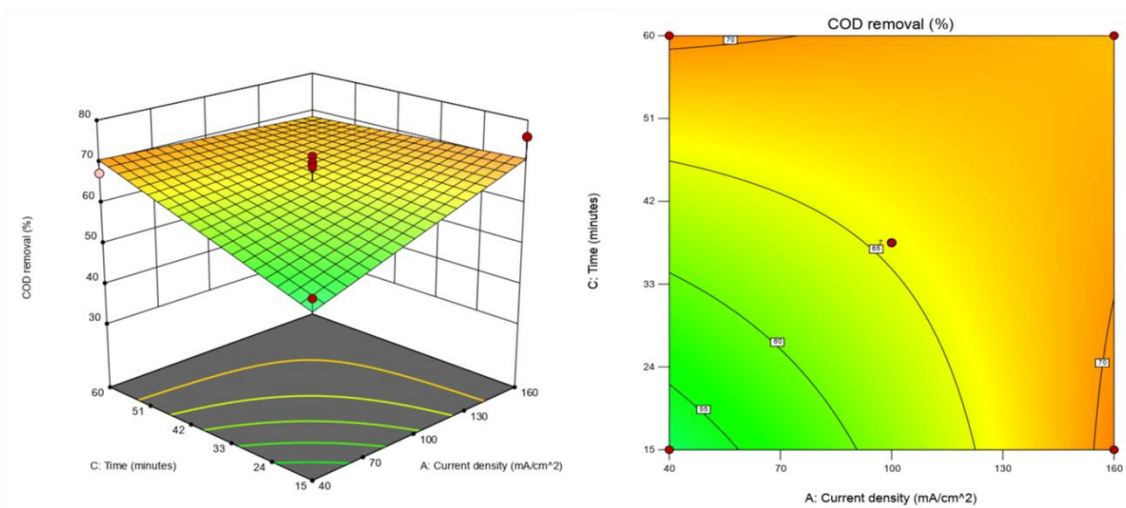


**Fig. 4.** 3D surface and contour plots showing the combined effect of time and current density on COD removal

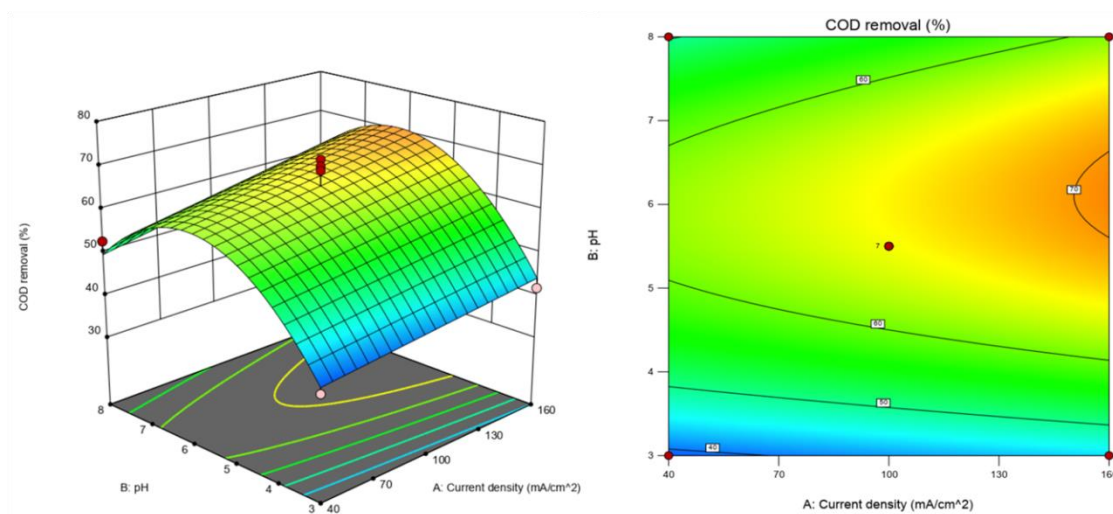


**Fig. 5.** 3D surface and contour plots showing the combined effect of current density and initial pH on COD removal

Current density is a crucial factor that influences the reaction rate of the EC process (Sher et al., 2020). It promotes the formation of coagulant quantity and hydrogen bubble formation, floc size and growth for pollutant removal (Nasrullah et al., 2020). In this work, the effect of applied current on COD removal efficiency was monitored at a range of current density (40-160 mA/cm<sup>2</sup>) for the treatment of synthetic BPOME. The maximum COD was removed at the current density of 160 mA/cm<sup>2</sup>. Increasing the current density resulted in a greater COD removal as also reported by (Kobyas et al., 2006; Manilal et al., 2020). As the current density was raised from 40 to 160 mA/cm<sup>2</sup>, the COD % removal increased up to 71.5%. This was due to the increased release of aluminium ions in electrolytic oxidation and hydroxide formation that enhanced the coagulation activity and subsequent precipitation, corresponding to the increase in applied current (Shankar et al., 2014). Even though a higher current density enhances the EC process efficiency, after a certain period of time, the removal efficiency drops due to over occupied active sites of the coagulant-pollutant complex (Lekhlif et al., 2014) and destabilization of the pollutant adsorption (Foudhaili et al., 2020). According to the general Faraday's law, the removal efficiency increases with increasing reaction time, as multiple ion hydroxide complexes are produced to entrap the colloidal pollutants. However, a peak point is reached when the EC removal efficiency does not further increase as the complexes reach a saturation point (Loukanov et al., 2020).

Hence, a mutual interaction of both current density and time has shown a combined effect on the final COD removal % and is evidently reflected in the ANOVA analysis of the quadratic model. The synergistic effect of the parameter interaction on COD removal % was proven to be statistically significant in this study with a *p*-value of 0.0043. The EC process in this study was varied from 15 to 60 minutes. With 160 mA/cm<sup>2</sup> current density i.e. 1.75 A of applied current in this study, the optimum COD removal % was achieved in 15 minutes. Increased current density corresponds with reduced reaction time (Sharma et al., 2020). Though a lower current density promotes reduced power consumption, the overall process is compensated with overall higher time duration required to achieve the optimum pollutant removal % (Wagle et al., 2019).

As EC process progresses, heat released in the electrolytic redox reactions raise the reactor temperature, as observed in this study. Although the heat released was considered negligible in this work, the consequences of possible excessive heat production in large scale EC operation in the industrial scale is a concern. Studies by El-Ashtoukhy et al. (2008) and Sekar et al. (2004) recommend determination of optimum current density to minimize undesirable effect of heat generation.

Moreover, with increased current density, a higher rate of hydrogen bubbles on the surface of the working mixture was observed. This phenomenon corresponds to the increased rate of anode dissociation with high current density (Moussa et al., 2017; Tahreen et al., 2020). It was also reported that current density influences the bubble size along with bubble quantity (Fukui & Yuu, 1985). The release of hydrogen as bubbles at the cathode tend to produce bubble turbulence in the reactor that affects the floc formation (Loukanov et al., 2020).

As per electrolysis of water, production of 1 mol of H<sub>2</sub> corresponds with 2 moles of electrons. The correlation among bubble velocity, gas-flow rate and current intensity was derived in the study by (Bannari et al., 2019), and is presented in equation (4), where  $U_g$  (m/s) is the superficial bubble velocity,  $Q_G$  is the gas volume flow-rate,  $S_e$  is the electrode surface area (cm<sup>2</sup>),  $M_{H_2}$  is the molar mass of H<sub>2</sub> (2.016 g/mol),  $\rho_G$  is the H<sub>2</sub> density (0.085 kg/m<sup>3</sup>) and  $F$  is the Faraday's constant (96500 C/mol).

$$U_g = \frac{Q_G}{S_e} = \frac{IM_{H_2}}{2F\rho_G S_e} \quad (4)$$

With a current of 1.75 A, and  $S_e$  of 10.93 cm<sup>2</sup> in this work, the H<sub>2</sub> volume flow-rate,  $Q_G$ , was determined to be 2.15 x 10<sup>-7</sup> m<sup>3</sup>/s. Dividing  $Q_G$  with  $S_e$  gave 1.97 x 10<sup>-4</sup> m/s as the superficial velocity of H<sub>2</sub> bubbles in the EC reactor. With this bubble velocity at the highest current density (160 mA/cm<sup>2</sup>), at pH 6, the highest COD removal % was achieved in 15 minutes. Therefore, it was concluded that the bubble turbulence was not high enough to cause floc deformation that could affect the COD removal with the optimized parameters. This observation is in agreement with Bannari et al. (2019), where it was reported that, in order to prevent floc disintegration and support complete flotation, the hydrodynamic shear forces in the reactor should be weak (Bannari et al., 2019).

The perturbation plot in Figure 6 shows that the response of % COD removal is the most sensitive to changes in factor B (initial pH), which was also reported by (Akhtar et al., 2020). Numerous studies have reported that EC is sensitive to the initial pH of the wastewater as it controls the charge of the generated metal hydroxides that influence the removal efficiency (Garcia-Segura et al., 2017; Hashim et al., 2019; Naje et al., 2017; Sediqi et al., 2021). By varying the initial pH of the wastewater ranging from pH 3 to 8, the best COD removal % was obtained at pH 6 in this study. As EC progresses, Al<sup>3+</sup> ions are generated at anode and OH<sup>-</sup> ions at the cathode, the resulting aluminium hydroxides undergo speciation depending on the pH of the electrochemical solution and wastewater under treatment (Sardari et al., 2018). In the pH range of 6 to 8, amorphous Al(OH)<sub>3</sub> species with large surface area are prevalent (Gheraout et al., 2015; Shankar et al., 2014). The Al(OH)<sub>3</sub> as gelatinous suspension removes the organics and suspended solids from the wastewater by means of complex formation, electrostatic attraction, followed by coagulation and flocculation (Gheraout et al., 2009). However, in a more alkaline pH, Al hydroxides prevail in a negatively charged species of Al(OH)<sub>4</sub><sup>-</sup> and charge repulsion restricts complexation and adsorption of pollutants (Sardari et al., 2018). Therefore, in this work, the optimum amount of coagulants produced to remove optimum COD % was at pH 6.

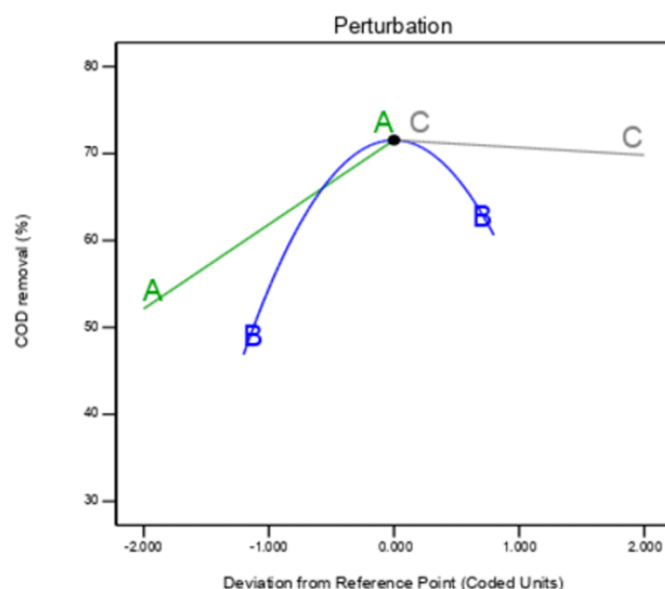
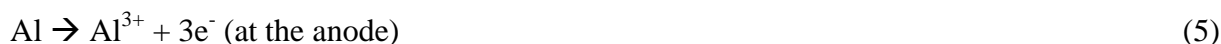


**Fig. 6.** Perturbation plot of COD removal (%).

As a sacrificial electrode, aluminium anode loses its mass over time while releasing aluminium ions and electrons in the electrolytic solution, while hydrogen bubbles are released at the cathode with the production of hydroxide ions. The SEM image of aluminium anode

depicts anomalous floccules on its porous surface, as shown in Figure 7. The porous anode represents the loss of aluminium ions during anode dissociation in EC. Similar anode structure of Al had also been observed and reported by (Hashim et al., 2019). The redox reactions that govern the dissociation of aluminium anode to release  $\text{Al}^{3+}$  ions for EC are presented in equations (5) and (6).



Using the Faraday's equation as in (Holt et al., 2002), the theoretical amount of total aluminium utilized was determined to be 0.839 g and 4.20 g/L in terms of concentration, at the current density of 160 mA/cm<sup>2</sup> at 1.75 A, pH 6 and 15 minutes of EC treatment. Electrode loss and requirement of periodic anode replacement stands out as a downfall of the EC process. But the continuous effective release of coagulant in situ with simplicity and without external chemical addition, and quick treatment results, surpass the disadvantage.

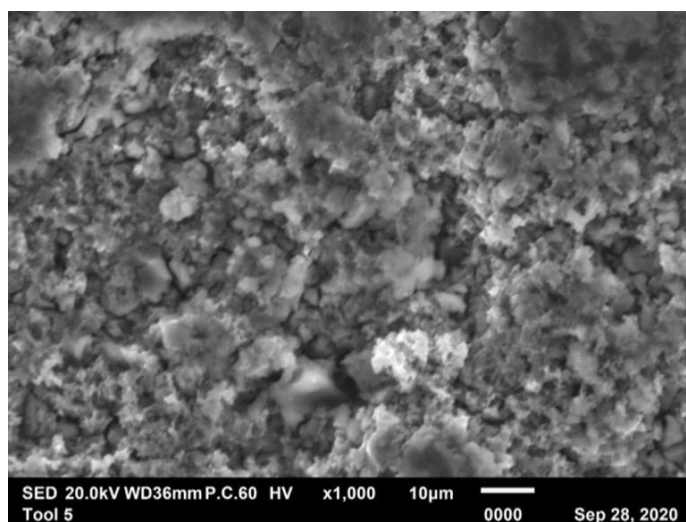


**Fig. 7.** SEM image of aluminium anode after EC.

The EC process was validated with real BPOME with the optimized parameters from EC on synthetic wastewater. The BPOME was collected from the final discharge pond released at the capacity of 23 tons per hour in Negeri Sembilan based palm oil mill, Malaysia. The BPOME samples were brown in colour with high notable turbidity. The collected effluent was stored in 4°C and characterized according to APHA standards, presented in Table 5.

**Table 5.** Characterization of BPOME

Parameters	Average values
COD (mg/L)	1981
TSS (mg/L)	192
Colour (PtCo)	2882
Salinity (ppt)	8.2
TDS (g/L)	7.91
Conductivity (mS/cm)	14.1
pH	7.90
Turbidity (NTU)	332

Despite storing at 4°C temperature, the BPOME samples depicted a very slight degradation in its parameters especially COD, TSS, turbidity and colour overtime, as a result of natural biodegradation (Mohd-Nor et al., 2019). Therefore, the characterization of the sample was recorded as average values considering the values previously noted and the reading during the experiment.

For both synthetic and real BPOME, EC did not have any significant effect on the TDS, conductivity and salinity levels, but notably differed in COD, turbidity, TSS, and colour values. The final treated solution was a transparent yellow solution with 0.3 NTU turbidity and 0 mg/L of TSS. The validation with real BPOME with the optimized current density resulted in 60.7 % COD, 99.91 % turbidity, 100 % TSS, and 95.7 % colour removal after 15 minutes of EC. The parameters denoting the pollutant removal efficiency are presented in Table 6.

**Table 6.** Characterization of EC treated BPOME.

Parameters	Value	Average removal efficiency
COD (mg/L)	779±1	60.7 %
TSS (mg/L)	0	100 %
Colour (PtCo)	123	95.7 %
Turbidity (NTU)	0.3	99.91 %

Even though the COD removal with EC differed between the real BPOME and synthetic wastewater, the turbidity, TSS and turbidity were removed nearly to completion in BPOME, in just 15 minutes of operation without addition of any electrolytes. The electrical conductivity of BPOME samples was high enough to run the highest current density considered in this study, compared to the synthetic wastewater. As the real BPOME is more complex with the presence of various proteins and organic substances, the slight gap in COD removal % prevails, compared to the same treatment on the synthetic wastewater with the same optimized parameters. However, the effect of additional supporting electrolytes on real BPOME on EC pollutant removal efficiency is worth exploring.

## CONCLUSION

Using aluminium electrodes with inter electrode distance of 10 mm and working volume of 200 ml of synthetic wastewater, and a range of initial pH, current density and time of 3-8, 40-160 mA/cm<sup>2</sup> and 15 to 60 minutes, respectively, the three critical variables were optimized using Design Expert Software version 13.0. With BBD under RSM, the highest COD removal of 71.5% was determined at pH 6, current density of 160 mA/cm<sup>2</sup> (with 1.75 A) and EC time of 15 minutes. At optimum conditions, beside COD, 99.68% TSS, 99.39 % turbidity and 97.95% colour were also removed from EC stand-alone treatment. A higher current density drastically reduced the EC time, and adding supporting electrolytes required comparatively less voltage to achieve the desired current density. Also, it was observed that the initial pH significantly impacts the COD removal in the EC process. After optimization, the synergistic impact of the combined critical parameters propels this field in terms of leveraging the parameter interaction to produce sustainable outcome in the palm oil mill industry. The verification experiments with real BPOME with the optimized parameters resulted in the removal of 60.7 % COD, 99.91% turbidity, 100 % TSS, and 95.7 % colour, which was impressive for a short reaction time of 15 minutes without the addition of any supporting

electrolytes. Therefore, EC displays promising potential for cleaner industrial discharge and is worth further exploring to contribute a complete sustainable water reclamation system.

## ACKNOWLEDGEMENT

The authors express thanks to International Islamic University Malaysia, Faculty of Engineering, for the financial support under Tuition Fee Waiver (TFW) 2019 scheme.

## GRANT SUPPORT DETAILS

The authors express their gratitude to Ministry of Education (MOE) Malaysia for granting a Fundamental Research Grant Scheme (FRGS), project no. FRGS-19-194-0803 to support this work.

## CONFLICT OF INTEREST

The authors declare that there is not any conflict of interests regarding the publication of this manuscript. In addition, the ethical issues, including plagiarism, informed consent, misconduct, data fabrication and/ or falsification, double publication and/or submission, and redundancy has been completely observed by the authors.

## LIFE SCIENCE REPORTING

No life science threat was practiced in this research.

## REFERENCES

- Abdulazeez, Q. M., Jami, M. S. and Alam, M. Z. (2018). Feasibility of using kaolin suspension as synthetic sludge sample. *J. Adv. Res. Fluid Mech. Therm. Sci.*, 48; 25–39.
- Akarsu, C., Ozay, Y., Dizge, N., Gulsen, H. E., Ates, H., Gozmen, B. and Turabik, M. (2016). Electrocoagulation and nanofiltration integrated process application in purification of bilge water using response surface methodology. *Water Sci. Technol.*, 74(3); 564–579.
- Akhtar, A., Aslam, Z., Asghar, A., Bello, M. M. and Raman, A. A. A. (2020). Electrocoagulation of Congo Red dye-containing wastewater: Optimization of operational parameters and process mechanism. *J. Environ. Chem. Eng.*, 8(5); 104055.
- Amosa, M. K., Jami, M. S., Alkhatib, M. F. R. and Majozi, T. (2016). Studies on pore blocking mechanism and technical feasibility of a hybrid PAC-MF process for reclamation of irrigation water from biotreated POME. *Sep. Sci. Technol.*, 51(12); 2047–2061.
- APHA, American Public Health Association (2002). American Water Works Association, Water Environment Federation; Stand. Methods Exam. Water Wastewater.
- Aslan, A. K. H. N., Ali, M. D. M., Morad, N. A. and Tamunaidu, P. (2016). Polyhydroxyalkanoates production from waste biomass. *IOP Conf. Ser.: Earth Environ. Sci.*, 36(1); 012040.
- Aswathy, P., Gandhimathi, R., Ramesh, S. T. and Nidheesh, P. V. (2016). Removal of organics from bilge water by batch electrocoagulation process. *Sep. Purif. Technol.*, 159; 108–115.
- Bahadur, N. and Bhargava, N. (2019). Novel pilot scale photocatalytic treatment of textile & dyeing industry wastewater to achieve process water quality and enabling zero liquid discharge. *J. Water Process Eng.*, 32; 100934.
- Bannari, R., Hilali, Y., Essadki, A. and Bannari, A. (2019). Computational fluid dynamic for improving design and performance of an external loop airlift reactor used in electrochemical wastewater treatment. *SN Appl. Sci.*, 1(11); 1–17.

- Bashir, M. J., Lim, J. H., Abu Amr, S. S., Wong, L. P. and Sim, Y. L. (2019). Post treatment of palm oil mill effluent using electro-coagulation-peroxidation (ECP) technique. *J. Clean. Prod.*, 208; 716–727.
- Boczkaj, G. and Fernandes, A. (2017). Wastewater treatment by means of advanced oxidation processes at basic pH conditions: A review. *Chem. Eng. J.*, 320; 608–633.
- Chavalparit, O. and Ongwandee, M. (2009). Optimizing electrocoagulation process for the treatment of biodiesel wastewater using response surface methodology. *J. Environ. Sci.*, 21(11); 1491–1496.
- Deveci, E. Ü., Akarsu, C., Gönen, Ç. and Özay, Y. (2019). Enhancing treatability of tannery wastewater by integrated process of electrocoagulation and fungal via using RSM in an economic perspective. *Process Biochem.*, 84; 124–133.
- Dimoglo, A., Sevim-Elibol, P., Dinç, Gökmen, K. and Erdoğan, H. (2019). Electrocoagulation/electroflotation as a combined process for the laundry wastewater purification and reuse. *J. Water Process Eng.*, 31;100877.
- El-Ashtoukhy, E. S. Z., Amin, N. K. and Abdelwahab, O. (2008). Removal of lead (II) and copper (II) from aqueous solution using pomegranate peel as a new adsorbent. *Desalin.*, 223; 162–173.
- Foudhaili, T., Lefebvre, O., Coudert, L. and Neculita, C. M. (2020). Sulfate removal from mine drainage by electrocoagulation as a stand-alone treatment or polishing step. *Miner. Eng.*, 152; 106337.
- Fukui, Y. and Yuu, S. (1985). Removal of colloidal particles in electroflotation. *AIChE J.*, 31(2); 201–208.
- Garcia-Segura, S., Eiband, M. M. S. G., de Melo, J. V. and Martínez-Huitle, C. A. (2017). Electrocoagulation and advanced electrocoagulation processes: A general review about the fundamentals, emerging applications and its association with other technologies. *J. Electroanal. Chem.*, 801; 267–299.
- Ghernaout, D., Ghernaout, B., Boucherit, A., Naceur, M. W., Khelifa, A. and Kellil, A. (2009). Study on mechanism of electrocoagulation with iron electrodes in idealised conditions and electrocoagulation of humic acids solution in batch using aluminium electrodes. *Desalin. Water Treat.*, 8(1–3); 91–99.
- Ghernaout, Djamel, Al-Ghonamy, A. I., Ait Messaoudene, N., Aichouni, M., Naceur, M. W., Benchelighem, F. Z. and Boucherit, A. (2015). Electrocoagulation of Direct Brown 2 (DB) and BF Cibacete Blue (CB) using aluminum electrodes. *Sep. Sci. Technol.*, 50(9); 1413–1420.
- Hashim, K. S., Jasim, N., Shaw, A., Phipps, D., Kot, P., Alattabi, A. W., Abdulredha, M. and Alawsh, R. (2019). Electrocoagulation as a green technology for phosphate removal from river water. *Sep. Purif. Technol.*, 210; 135–144.
- Holt, P. K., Barton, G. W., Wark, M. and Mitchell, C. A. (2002). A quantitative comparison between chemical dosing and electrocoagulation. *Colloids Surfaces A Physicochem. Eng. Asp.*, 211(2–3); 233–248.
- Hussin, F., Abnisa, F., Issabayeva, G., & Aroua, M. K. (2017). Removal of lead by solar-photovoltaic electrocoagulation using novel perforated zinc electrode. *J. Clean. Prod.*, 147; 206–216.
- Ilyas, A., Mertens, M., Oyaert, S. and Vankelecom, I. F. J. (2020). Synthesis of patterned PVDF ultrafiltration membranes: Spray-modified non-solvent induced phase separation. *J. Memb. Sci.*, 612; 118383.
- Iskandar, M. J., Baharum, A., Anuar, F. H. and Othaman, R. (2018). Palm oil industry in South East Asia and the effluent treatment technology—A review. *Environ. Technol. Innov.*, 9; 169–185.
- Jawad, A. H., Rashid, R. A., Ishak, M. A. M. and Wilson, L. D. (2016). Adsorption of methylene blue onto activated carbon developed from biomass waste by H<sub>2</sub>SO<sub>4</sub> activation: kinetic, equilibrium and thermodynamic studies. *Desalin. Water Treat.*, 57(52); 25194–25206.
- Jayakaran, P., Nirmala, G. S. and Govindarajan, L. (2019). Qualitative and quantitative analysis of graphene-gased adsorbents in wastewater treatment. *Int. J. Chem. Eng.*, 2019.
- Khosravi, R., Hossini, H., Heidari, M., Fazlzadeh, M., Biglari, H., Taghizadeh, A. and Barikbin, B. (2017). Electrochemical decolorization of reactive dye from synthetic wastewater by mono-polar aluminum electrodes system. *Int. J. Electrochem. Sci.*, 12(6); 4745–4755.

- Koby, M., Hiz, H., Senturk, E., Aydiner, C. and Demirbas, E. (2006). Treatment of potato chips manufacturing wastewater by electrocoagulation. *Desalin.*, 190(1–3); 201–211.
- Lekhlif, B., Oudrhiri, L., Zidane, F., Drogui, P. and Blais, J. F. (2014). Study of the electrocoagulation of electroplating industry wastewaters charged by nickel (II) and chromium (VI). *J. Mater. Environ. Sci.*, 5(1); 111–120.
- Loukanov, A., El Allaoui, N., Omor, A., Elmadani, F. Z., Bouayad, K. and Seiichiro, N. (2020). Large-scale removal of colloidal contaminants from artisanal wastewater by bipolar electrocoagulation with aluminum sacrificial electrodes. *J. Neurol. Sci.*, 2; 100038.
- Manilal, A. M., Soloman, P. A., & Basha, C. A. (2020). Removal of Oil and Grease from Produced Water Using Electrocoagulation. *J. Hazardous, Toxic, Radioact. Waste*, 24(1).
- McBeath, S. T., Nouri-Khorasani, A., Mohseni, M., & Wilkinson, D. P. (2020). In-situ determination of current density distribution and fluid modeling of an electrocoagulation process and its effects on natural organic matter removal for drinking water treatment. *Water Res.*, 171.
- Mohd-Nor, D., Ramli, N., Sharuddin, S. S., Hassan, M. A., Mustapha, N. A., Ariffin, H., Sakai, K., Tashiro, Y., Shirai, Y., & Maeda, T. (2019). Dynamics of microbial populations responsible for biodegradation during the full-scale treatment of palm oil mill effluent. *Microbes Environ.*, 34(2); 121–128.
- Moussa, D. T., El-Naas, M. H., Nasser, M. and Al-Marri, M. J. (2017). A comprehensive review of electrocoagulation for water treatment: Potentials and challenges. *J. Environ. Manage.*, 186; 24–41.
- Naje, A. S., Chelliapan, S., Zakaria, Z., Ajeel, M. A. and Alaba, P. A. (2017). A review of electrocoagulation technology for the treatment of textile wastewater. *Rev. Chem. Eng.*, 33(3); 263–292.
- Nasrullah, M., Singh, L., Krishnan, S., Sakinah, M., Mahapatra, D. M. and Zularisam, A. W. (2020). Electrocoagulation treatment of raw palm oil mill effluent: Effect of operating parameters on floc growth and structure. *J. Water Process Eng.*, 33; 101114.
- Nasrullah, M., Singh, L., Mohamad, Z., Norsita, S., Krishnan, S., Wahida, N. and Zularisam, A. W. (2017). Treatment of palm oil mill effluent by electrocoagulation with presence of hydrogen peroxide as oxidizing agent and polialuminum chloride as coagulant-aid. *Water Resour. Ind.*, 17; 7–10.
- Nopens, I., Capalozza, C. and Vanrolleghem, P. A. (2001) Stability analysis of a synthetic municipal wastewater. Dissertation, Ghent University.
- Reilly, M., Cooley, A. P., Tito, D., Tassou, S. A. and Theodorou, M. K. (2019). Electrocoagulation treatment of dairy processing and slaughterhouse wastewaters. *Energy Procedia*, 161; 343–351.
- Rusdianasari, Taqwa, A., Jaksen and Syakdani, A. (2017). Treatment optimization of electrocoagulation (EC) in purifying palm oil mill effluents (POMEs). *J. Eng. Technol. Sci.*, 49(5); 604–617.
- Sandoval, M. A., Fuentes, R., Thiam, A., & Salazar, R. (2021). Arsenic and fluoride removal by electrocoagulation process: A general review. *Sci. Total Environ.*, 753; 142108.
- Sardari, K., Fyfe, P., Lincicome, D. and Wickramasinghe, S. R. (2018). Aluminum electrocoagulation followed by forward osmosis for treating hydraulic fracturing produced waters. *Desalin.*, 428; 172–181.
- Sediqi, S., Bazargan, A., & Mirbagheri, S. A. (2021). Consuming the least amount of energy and resources in landfill leachate electrocoagulation. *Environ. Technol. Innov.*, 22; 101454.
- Sekar, M., Sakthi, V. and Rengaraj, S. (2004). Kinetics and equilibrium adsorption study of lead(II) onto activated carbon prepared from coconut shell. *J. Colloid Interface Sci.*, 279(2); 307–313.
- Shankar, R., Singh, L., Mondal, P. and Chand, S. (2014). Removal of COD, TOC, and color from pulp and paper industry wastewater through electrocoagulation. *Desalin. Water Treat.*, 52(40–42); 7711–7722.
- Sharma, S., Aygun, A. and Simsek, H. (2020). Electrochemical treatment of sunflower oil refinery wastewater and optimization of the parameters using response surface methodology. *Chemosphere*, 249; 126511.

- Sher, F., Hanif, K., Zafar, S. and Imran, M. (2020). Implications of advanced wastewater treatment : Electrocoagulation and electroflocculation of effluent discharged from a wastewater treatment plant. *J. Water Process Eng.*, 33.
- Tahreen, A. and Jami, M. S. (2021). Advances in antifouling strategies in membrane ultrafiltration : A brief review. *J. Adv. Res. Mater. Sci.*, 1(1); 10–16.
- Tahreen, A., Jami, M. S. and Ali, F. (2020). Role of electrocoagulation in wastewater treatment: A developmental review. *J. Water Process Eng.*, 37; 101440.
- Thakur, L. S., Goyal, H. and Mondal, P. (2019). Simultaneous removal of arsenic and fluoride from synthetic solution through continuous electrocoagulation: Operating cost and sludge utilization. *J. Environ. Chem. Eng.*, 7(1).
- UN. (2018). SDG 6 Synthesis Report 2018 on Water and Sanitation.
- Wagle, D., Lin, C., Nawaz, T. and Shipley, H. J. (2019). Evaluation and optimization of electrocoagulation for treating Kraft paper mill wastewater. *Biochem. Pharmacol.*, 8(1); 103595.
- WEF. (2020). World Economic Forum. The Global Risks Report 2020 Insight Report, 15.
- Zaied, B. K., Rashid, M., Nasrullah, M., Zularisam, A. W., Pant, D., & Singh, L. (2020). A comprehensive review on contaminants removal from pharmaceutical wastewater by electrocoagulation process. *Sci. Total Environ.*, 726; 138095.

